

Regulation of Axon Guidance by Compartmentalized Nonsense-Mediated mRNA Decay

Dilek Colak,¹ Sheng-Jian Ji,¹ Bo T. Porse,^{2,3,4} and Samie R. Jaffrey^{1,*}

¹Department of Pharmacology, Weill Medical College, Cornell University, New York, NY 10065, USA

²The Finsen Laboratory, Rigshospitalet, Faculty of Health Sciences

³Biotech Research and Innovation Center (BRIC)

⁴Danish Stem Cell Centre (DanStem), Faculty of Health Sciences

University of Copenhagen, Copenhagen 2200, Denmark

*Correspondence: srj2003@med.cornell.edu

<http://dx.doi.org/10.1016/j.cell.2013.04.056>

SUMMARY

Growth cones enable axons to navigate toward their targets by responding to extracellular signaling molecules. Growth-cone responses are mediated in part by the local translation of axonal messenger RNAs (mRNAs). However, the mechanisms that regulate local translation are poorly understood. Here we show that Robo3.2, a receptor for the Slit family of guidance cues, is synthesized locally within axons of commissural neurons. *Robo3.2* translation is induced by floor-plate-derived signals as axons cross the spinal cord midline. *Robo3.2* is also a predicted target of the nonsense-mediated mRNA decay (NMD) pathway. We find that NMD regulates *Robo3.2* synthesis by inducing the degradation of *Robo3.2* transcripts in axons that encounter the floor plate. Commissural neurons deficient in NMD proteins exhibit aberrant axonal trajectories after crossing the midline, consistent with misregulation of *Robo3.2* expression. These data show that local translation is regulated by mRNA stability and that NMD acts locally to influence axonal pathfinding.

INTRODUCTION

Nonsense-mediated mRNA decay (NMD) is a mechanism that regulates protein expression by controlling the stability of specific transcripts (Doma and Parker, 2007; Hodgkin et al., 1989; Leeds et al., 1992). NMD was initially identified as a pathway that degrades transcripts containing mutations or DNA rearrangements that result in a premature stop codon (Lejeune and Maquat, 2005; Li and Wilkinson, 1998; Maquat et al., 1981). NMD is triggered when a ribosome at the stop codon detects downstream mRNA-bound proteins that participate in splicing reactions. After splicing reactions, a complex of proteins involved in splicing remain bound at the junction between each exon. In most transcripts, all exon-junction complexes are up-

stream of the stop codon and are removed during the initial rounds of translation (Chang et al., 2007; Dostie and Dreyfuss, 2002; Ishigaki et al., 2001). However, in the case of mutations that result in a new stop codon, some exon-junction complexes might be present downstream of the stop codon. This initiates a process that ultimately leads to mRNA degradation (Carter et al., 1995; Zhang et al., 1998).

Recent findings have suggested that NMD may have broader roles in regulating mRNA and protein expression. In some cases, endogenously expressed transcripts appear to be NMD targets due to introns in the 3' UTR or alternative splicing events that result in a stop codon that is followed by an exon-junction complex (Giorgi et al., 2007; McGlinchey and Smith, 2008; Weischenfeldt et al., 2012; Zheng et al., 2012). NMD appears to regulate the stability of both of these types of transcripts, thereby affecting the levels of the translated protein. However, the extent to which the NMD-dependent degradation of these transcripts is physiologically relevant is not clear.

An example of a transcript that has important physiological roles and is also a predicted NMD target is *Robo3.2* (Black and Zipursky, 2008). The *Robo3.2* isoform differs from *Robo3.1* by the presence of a retained intron resulting in a new stop codon that is upstream of an exon-junction complex. As a result, *Robo3.2* is a predicted NMD target.

During commissural axon guidance in the spinal cord, axons are initially attracted to and, upon crossing, become repulsed from the ventral midline. These sequential events are governed by guidance cues released from the floor plate, which is a region of specialized glial cells in the midline (Long et al., 2004; O'Donnell et al., 2009; Serafini et al., 1994). The precise regulation of the spatiotemporal expression of *Robo3.1* and *Robo3.2*, which are alternatively spliced forms of *Robo3*, is critical for the proper guidance of commissural axons (Chen et al., 2008). As the axons grow toward the midline, they express *Robo3.1* but not *Robo3.2*, although the *Robo3.2* transcript is abundant in commissural neurons (Chen et al., 2008). However, after the commissural axons have crossed through the midline, *Robo3.2* protein is induced and selectively detected in the postcrossing axonal segment, and *Robo3.1* protein is downregulated (Chen et al., 2008). *Robo3.1* allows axons to approach the midline by suppressing

the activity of Robo1 and Robo2, which otherwise mediate repulsion from the midline. Following midline crossing, axons are repelled from the midline due to the loss of Robo3.1 and the expression of Robo3.2; this supports the activity of Robo1 and Robo2 (Chen et al., 2008). The mechanism that controls the compartmentalized expression of Robo3.2 is not known.

Recent studies have identified local translation as a mechanism that controls growth-cone responses to axon-guidance cues (Campbell and Holt, 2001; Jung et al., 2012; Leung et al., 2006). During embryonic development, a small subset of cellular mRNAs are trafficked into axons and locally translated (Campbell and Holt, 2001; Jung et al., 2012; Tennyson, 1970). Local translation affects the protein composition of growth cones, thereby affecting the responses to guidance cues. The mechanisms that regulate the expression levels of specific axonal transcripts are not fully understood.

Here we show that axon guidance is physiologically regulated by NMD. We show that the *Robo3.2* transcript is selectively trafficked to commissural axons and is translated when axons are exposed to floor-plate signals in the spinal-cord midline. Upon translation, *Robo3.2* transcripts are targeted by NMD, ultimately limiting *Robo3.2* protein levels in postcrossing axons. Selective deletion of the essential NMD component *Upf2* from commissural neurons results in elevated levels of *Robo3.2* protein in axons and aberrant postcrossing of axonal trajectories in the embryonic spinal cord. Additionally, we find that proteins that mediate NMD are highly enriched in growth cones from diverse neuronal types. These data demonstrate a role for NMD in influencing local translation pathways that regulate axon guidance and potentially other growth-cone functions.

RESULTS

Robo3.2 Protein Is Induced by Floor-Plate-Derived Signals

Throughout the different phases of commissural axon guidance, two alternatively spliced variants of the *Robo3* transcript, *Robo3.1* and *Robo3.2*, are expressed (Chen et al., 2008). Before axons cross through the spinal-cord midline, only *Robo3.1* protein is expressed, and no *Robo3.2* protein is detected despite the abundance of *Robo3.2* mRNA at this stage (Chen et al., 2008). However, after the axons cross the floor plate, *Robo3.2* protein is detected and seen exclusively in the postcrossing segment of these axons (Figure 1A, right panel).

A major difference between these two isoforms is that *Robo3.2* is a predicted NMD target. The *Robo3.2* isoform differs from *Robo3.1* by the presence of a retained intron. The *Robo3* gene contains 27 introns, which are all spliced out in *Robo3.1*. However, in *Robo3.2*, intron 26 is retained, resulting in the appearance of a new intron-derived stop codon (Figure 1A). An exon-junction complex, which derives from the splicing of intron 27, is downstream of the new stop codon in *Robo3.2*, which makes this isoform an NMD target. We therefore wondered whether NMD contributes to the precise spatiotemporal regulation of *Robo3.2* expression during axon guidance.

Because NMD targets transcripts when they are initially translated, we first wanted to establish how *Robo3.2* protein expres-

sion is induced. We considered two models: the expression of *Robo3.2* could be temporally programmed to coincide with the time when axons cross the midline (approximately embryonic day [E] 11), or the expression of *Robo3.2* could be induced when the axons encounter the floor plate. To address this, we used spinal-cord “half-open-book” explant cultures. Half-open-book explants were dissected from mouse embryos at E10.5, a time point before commissural axons have reached the floor plate.

We first sought to confirm that the half-open-book culture recapitulates axonal expression patterns that are floor plate dependent. Half-open-book explants were prepared in a way that each lateral half was harvested either with or without the floor plate (referred as +FP or -FP throughout the text, Figure 1B). Previous studies have utilized this system to examine floor-plate-dependent changes in axonal behavior (Zou et al., 2000). As expected, axons from -FP explants expressed TAG-1, a marker for precrossing axons (Figure S1A available online). These axons did not express postcrossing marker L1 (Figure S1A). However, axons from +FP explants no longer expressed TAG-1 but instead exhibited L1 staining (Figure S1A). These data indicate that the half-open-book culture recapitulates the expression patterns that are regulated by the floor plate *in vivo*.

We next examined whether the floor plate induces *Robo3.2* expression. *Robo3.2* levels were measured in half-open-book axons at days *in vitro* (DIV) 2 using a *Robo3.2*-specific antibody (Chen et al., 2008). *Robo3.2* staining was undetectable in -FP cultures, whereas *Robo3.2* was readily detected in axons of +FP cultures (Figure 1C). In contrast to *Robo3.2*, *Robo3.1* was detected in axons of -FP explants, whereas *Robo3.1* was not detectable in +FP cultures (Figures 1C and 1D). Thus, these data indicate that the expression of *Robo3.2* is induced by the floor plate.

We next asked whether the floor plate is sufficient to induce *Robo3.2* protein in commissural axons. To test this, we prepared conditioned medium from isolated floor-plate tissue (Nawabi et al., 2010) (Figure 1E). Application of floor-plate-conditioned medium (FCM) to -FP explants resulted in pronounced *Robo3.2* protein in axons, whereas control medium did not induce *Robo3.2* expression (Figure 1F). *Robo3.2* induction was most prominent at the most distal parts of the axons, suggesting that the regulatory pathways controlling *Robo3.2* expression may be enriched in distal axons (Figures 1G and 1H).

Intriguingly, *Robo3.2* protein was also induced in commissural cell bodies by FCM (Figure S1B). *In vivo*, *Robo3.2* expression is only seen in the postcrossing segments of commissural axons. The limited expression of *Robo3.2* *in vivo* supports the idea that the floor plate mediates local induction of *Robo3.2* as only the axons are exposed to floor plate *in vivo*. Taken together, these data show that the floor plate is necessary as well as sufficient for *Robo3.2* induction in commissural neurons.

***Robo3.2* mRNA Is Translationally Repressed prior to Midline Crossing**

We next asked whether the undetectable levels of *Robo3.2* protein in precrossing axons are due to degradation of *Robo3.2*

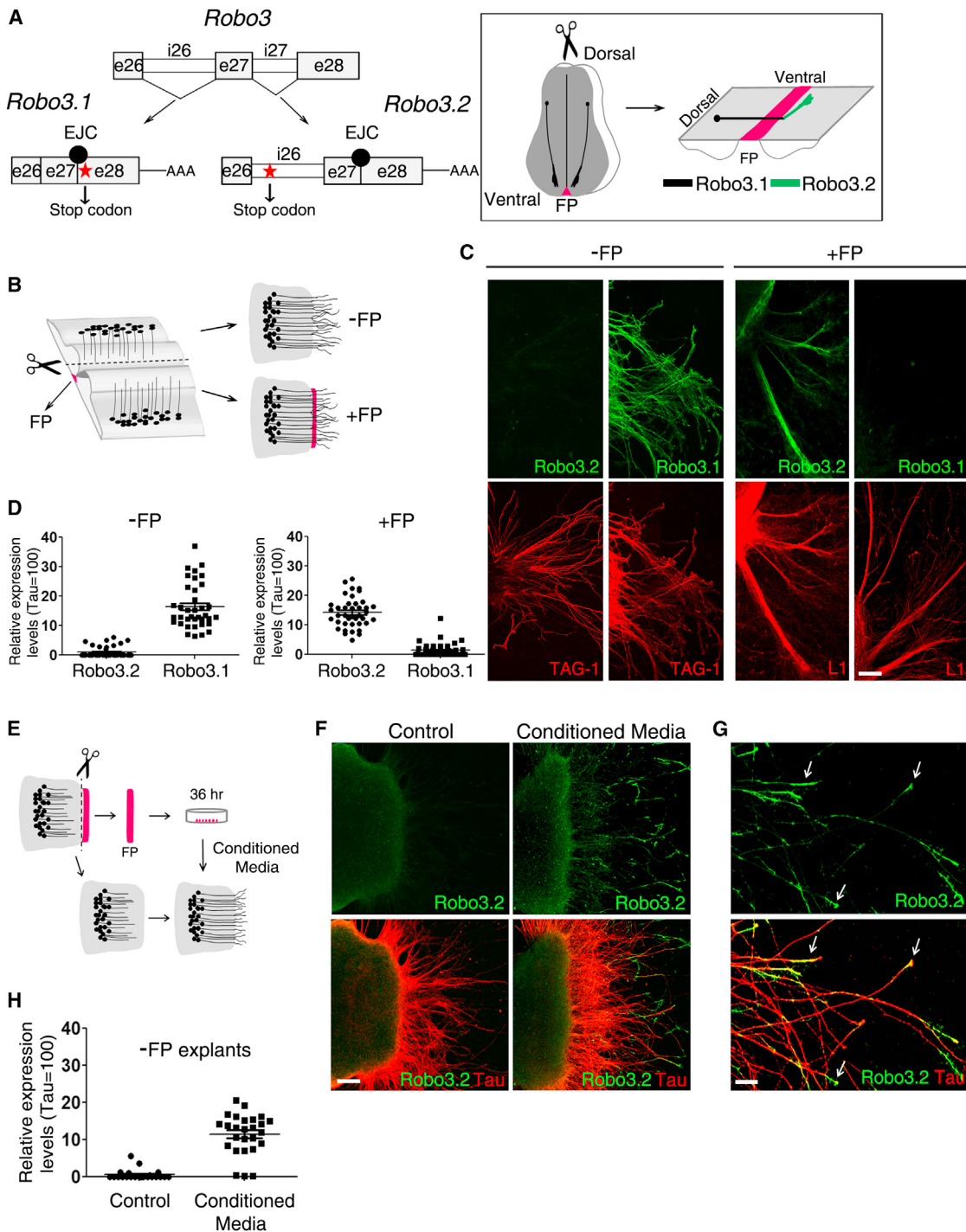


Figure 1. Robo3.2 Protein Levels Are Induced by Floor-Plate Signals

(A) Schematic representation of the *Robo3.2* transcript and *Robo3.2* expression pattern in spinal-cord commissural neurons. *Robo3.2* protein, green, is detected exclusively in the postcrossing segments of commissural axons.

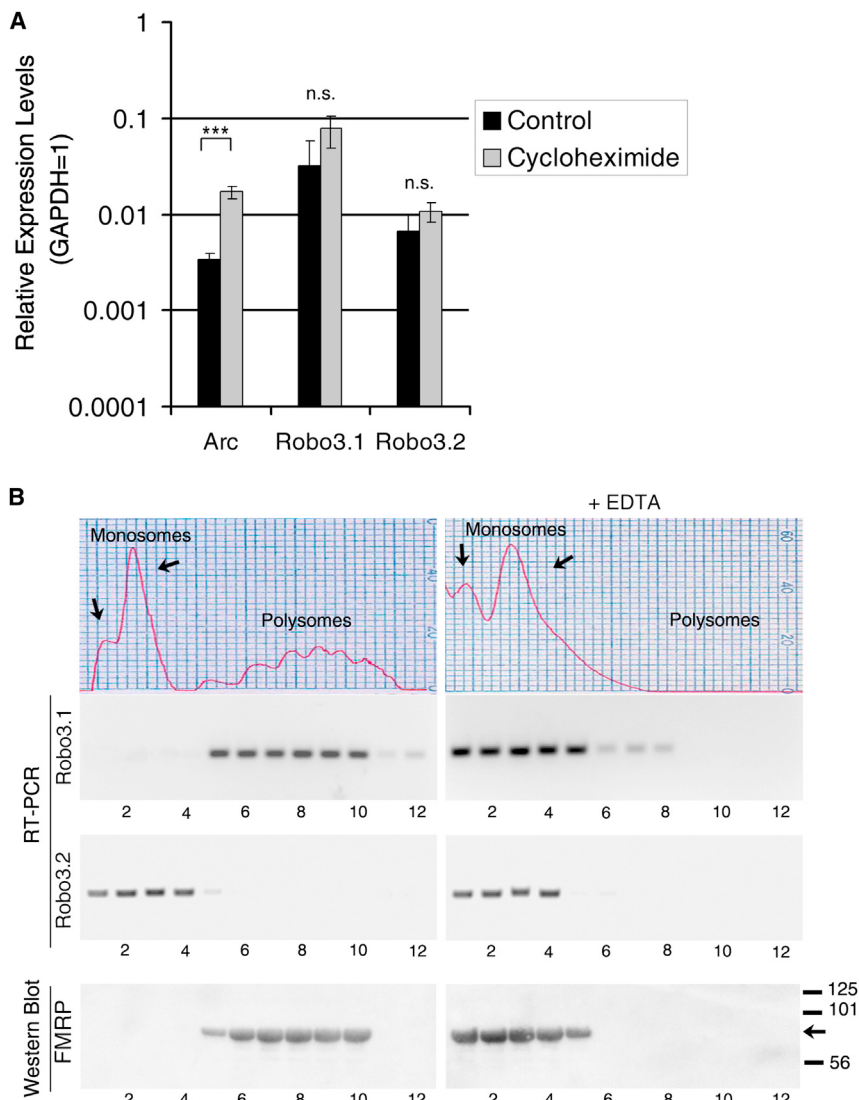
(B) Schematic of the half-open-book explant system. Half-open-book explants from E10.5 mouse spinal cords were cultured with (+FP) or without (-FP) the floor plate (indicated in pink).

(C and D) Immunostainings of *Robo3* isoforms in -FP and +FP explants. *Robo3.2* protein is detected only in +FP axons (C). (D) Quantification of results in (C) (*Robo3.2* staining: -FP, n = 41 explants, +FP, n = 42 explants; *Robo3.1* staining: -FP, n = 37, +FP, n = 40).

(E) Schematic of floor-plate-conditioned medium (FCM) experiment.

(F) FCM is sufficient to induce *Robo3.2* expression in precrossing axons (right panels).

(legend continued on next page)



mRNA by NMD. NMD targets are typically subjected to mRNA degradation. However, the *Robo3.2* transcript appears to be relatively abundant in commissural cells (Chen et al., 2008) (Figure S2A), which suggests that it escapes NMD in the cell body. Nevertheless, we asked whether NMD contributes to the stability of *Robo3.2* transcripts in precrossing neurons. A widely used approach to determine whether a transcript is subjected to NMD is to determine whether it accumulates after treatment of cells with cycloheximide, a protein synthesis inhibitor (Carter et al., 1995). This accumulation occurs because NMD-dependent RNA degradation requires protein translation (Ishigaki et al., 2001). We applied cycloheximide for 4 hr to -FP explants and used quantitative RT-PCR (qRT-PCR) to measure

Figure 2. *Robo3.2* mRNA Is Translationally Repressed prior to Midline Crossing

(A) *Robo3.2* is not a target of NMD in precrossing commissural neurons. qRT-PCR did not display a significant change in *Robo3.2* mRNA levels in cycloheximide-treated cells compared to untreated samples. NMD target *Arc* was increased 5-fold upon treatment with cycloheximide for 4 hr. Data are represented as mean \pm SEM, n = 3 biological replicates/condition, ***p < 0.001.

(B) *Robo3.2* is not translated in precrossing neurons. Polysome sedimentation was performed from E10.5 -FP explants. In addition to RNA absorbance profiles, FMRP immunoblotting was used as a marker for polysomes. *Robo3.2* mRNA was detected primarily in lighter fractions that are not associated with translating ribosomes. EDTA, which results in disruption of polysomes, re-localized FMRP and *Robo3.1* transcripts to the nontranslating fractions. The position of these markers is identical to the position of *Robo3.2*, confirming that *Robo3.2* mRNA is in nontranslating fractions.

See also Figure S2.

Robo3.2 levels in these explants. *Arc*, an established NMD target (Giorgi et al., 2007), was increased by 5-fold following cycloheximide treatment (Figure 2A). In contrast, *Robo3.2* levels were unaffected by this treatment (Figure 2A). Similarly, *Robo3.1*, which is not a predicted NMD target, was unaffected by cycloheximide treatment. These findings indicate that suppression of *Robo3.2* protein levels is not due to NMD at this developmental stage.

We next asked why *Robo3.2* is not subjected to NMD. Because NMD is dependent on translation, *Robo3.2* might escape NMD if it is not translated in precrossing neurons. To test this possibility, we isolated polysome-bound and polysome-free mRNAs by 10%–50% sucrose-gradient fractionation. FMRP, a marker of actively translating ribosomes, was selectively detected by western blotting in the polysome fractions (Figure 2B). Similarly, *Robo3.1* transcripts were detected by RT-PCR in the polysome fractions (Figure 2B). However, *Robo3.2* transcripts were only detected in the lighter fractions, which contain nontranslating mRNAs (Figure 2B). These data demonstrate that *Robo3.2* is translationally silenced in precrossing neurons.

As a further control, we asked whether *Robo3.2* protein is subjected to proteasomal degradation in precrossing neurons. To test this, we treated -FP explants with the proteasome

(G) High-power images depict prominent *Robo3.2* labeling at axonal tips (indicated by arrows).

(H) Quantification of *Robo3.2* levels following treatment with FCM (n = 26 explants) indicated a 10-fold increase in *Robo3.2* protein levels compared to untreated -FP axons (n = 23 explants).

Data represented as mean \pm standard error of the mean (SEM). Scale bars: (C and F) 150 μ m; (G) 60 μ m. See also Figure S1.

inhibitor MG-132. Treatment with proteasome inhibitors failed to increase Robo3.2 levels in –FP explants (Figure S2B). These data further indicate that the absence of Robo3.2 protein at this stage reflects translational suppression rather than a posttranslational mechanism.

Robo3.2 mRNA Is Transported into Precrossing and Postcrossing Axons

Because NMD occurs after a transcript is translated, we sought to determine how *Robo3.2* translation is initiated. Because *Robo3.2* expression is spatially restricted to postcrossing axons, and FCM results in highly selective expression of *Robo3.2* in distal axons, we considered the possibility that *Robo3.2* is locally translated (Figure 1F). We therefore first examined whether *Robo3.2* mRNA is localized to axons. Riboprobes directed against *Robo3.2* exhibited punctate localization along the axons, with enrichment toward the distal axons (Figures 3A–3D). This localization was seen in both pre- and postcrossing axons. Sense riboprobes and *Robo3.1*-specific riboprobes did not show signals in axons of either –FP or +FP explants (Figures S3A and S3B).

To further confirm that *Robo3.2* transcripts are localized to axons, we performed RT-PCR in isolated commissural axons (Figures 3E and 3F). To purify axons, we cultured explants in microfluidic chambers (Taylor et al., 2005). In these devices, explants are cultured in the cell-body compartment, and axons grow through a 450 μm microgroove barrier and appear in the axonal compartment by DIV4. Consistent with the fluorescence *in situ* hybridization (FISH) data, *Robo3.2* mRNA was detected by RT-PCR in both axons and cell bodies, whereas *Robo3.1* transcripts were only detected in cell bodies (Figure 3F). qRT-PCR data from isolated axonal samples further confirmed that *Robo3.2* mRNA is present in –FP and +FP axons (Figure 3G). These data demonstrate that *Robo3.2* mRNA is trafficked to axons before and after crossing the midline.

As in cell bodies, the undetectable levels of *Robo3.2* protein in precrossing axons were not due to NMD, given that selective treatment of axons with cycloheximide in microfluidic chambers did not result in an increase in *Robo3.2* mRNA levels in these axons (Figure S3C).

Robo3.2 Is Locally Translated in Postcrossing Axons

We next asked whether *Robo3.2* is translated in axons. To address this, we monitored *Robo3.2* levels after selectively inhibiting protein translation in axons. We cultured +FP explants in microfluidic chambers to fluidically isolate axons from cell bodies. This approach allows chemical treatments to only affect axons without affecting cell bodies (Cohen et al., 2011; Taylor et al., 2005). Selective application of cycloheximide to axons for 12 hr resulted in a nearly complete absence of *Robo3.2* expression (Figures 4A and 4B). These data support the idea that *Robo3.2* levels are regulated by local translation.

We next asked whether FCM induces the intra-axonal translation of *Robo3.2*. To test this, axons in –FP explant cultures were transected to prevent the possibility of transport of *Robo3.2* protein from the cell body and were treated with FCM (Figure 4C). Treatment of severed axons with FCM resulted in the appearance of *Robo3.2*, with particular enrichment in the distal parts

of the axons (Figure 4D). This effect was blocked by coapplication of cycloheximide, indicating that the induction of *Robo3.2* does not require the cell body and therefore is due to intra-axonal translation.

To further establish whether FCM induces translation of *Robo3.2* mRNA, we examined whether this treatment causes *Robo3.2* transcripts to shift to polysomes. Treatment of –FP explants with FCM resulted in the appearance of *Robo3.2* mRNA in polysomes (Figure S4A), indicating that *Robo3.2* is translationally derepressed upon exposure to floor-plate signals.

To determine whether contact to the floor plate itself induces *Robo3.2* synthesis in axons, we used half-open-book explants prepared from Wallerian degeneration slow (*Wld^S*) mice. The *Wld^S* mutant mouse contains a triplicate repeat of the *NMNAT-1* gene fused to the N-terminal domain of the ubiquitin ligase *UBE4* gene (Perry et al., 1991). Overexpression of *Wld^S* markedly delays axonal degeneration after axotomy (Feng et al., 2010). Because axons from *Wld^S* animals are viable following transection without exhibiting morphological signs of degeneration, they can be used to examine the role of local translation in isolated axons over prolonged periods. We cultured +FP explants from E10.5 *Wld^S* embryos and then cut the explants at DIV0.5 so that the cell bodies were severed from the axons (Figure 4E). Transected axons were capable of growing through the floor plate and inducing *Robo3.2* after crossing the midline in the absence of cell bodies (Figure 4F). As a control, we confirmed that the severing procedure removed the cell bodies from these explants (Figures S4B and S4C).

Taken together, these data indicate that *Robo3.2* translation occurs in axons in response to floor-plate signals. Because NMD-mediated degradation is translation dependent, this finding suggests that NMD-dependent regulation of *Robo3.2* mRNA would only occur in the postcrossing segment of commissural axons.

Robo3.2 Is Targeted for NMD upon Translational Derepression

In order to determine whether *Robo3.2* is potentially regulated by NMD, we next asked whether NMD machinery proteins are bound to *Robo3.2* transcripts. We used RNA immunoprecipitation (RIP) to examine the physical interaction of Upf1 and Upf2 with *Robo3.2* mRNA in +FP explants. mRNAs that are targeted by NMD have Upf2 bound to exon-junction complexes. Upf2-bound mRNAs trigger NMD by recruiting Upf1. Both Upf2 and Upf1 proteins interact with *Robo3.2* transcripts (Figure S5A), suggesting that *Robo3.2* mRNA is a potential NMD target in commissural neurons.

We next asked whether *Robo3.2* mRNA is subjected to NMD when commissural neurons begin to translate *Robo3.2* upon exposure to floor-plate signals. To address this, we used qRT-PCR to measure *Robo3.2* levels after treatment with FCM. Following treatment with FCM, *Robo3.2*-transcript levels were reduced by 70% in commissural cell bodies compared to treatment with control medium (Figure 5A). This effect was blocked by cycloheximide, suggesting that *Robo3.2* mRNA gets degraded following its translation induced by floor-plate signals (Figure 5A). Interestingly, *Robo3.1* levels drop upon FCM treatment. This is expected because *Robo3.1* mRNA is

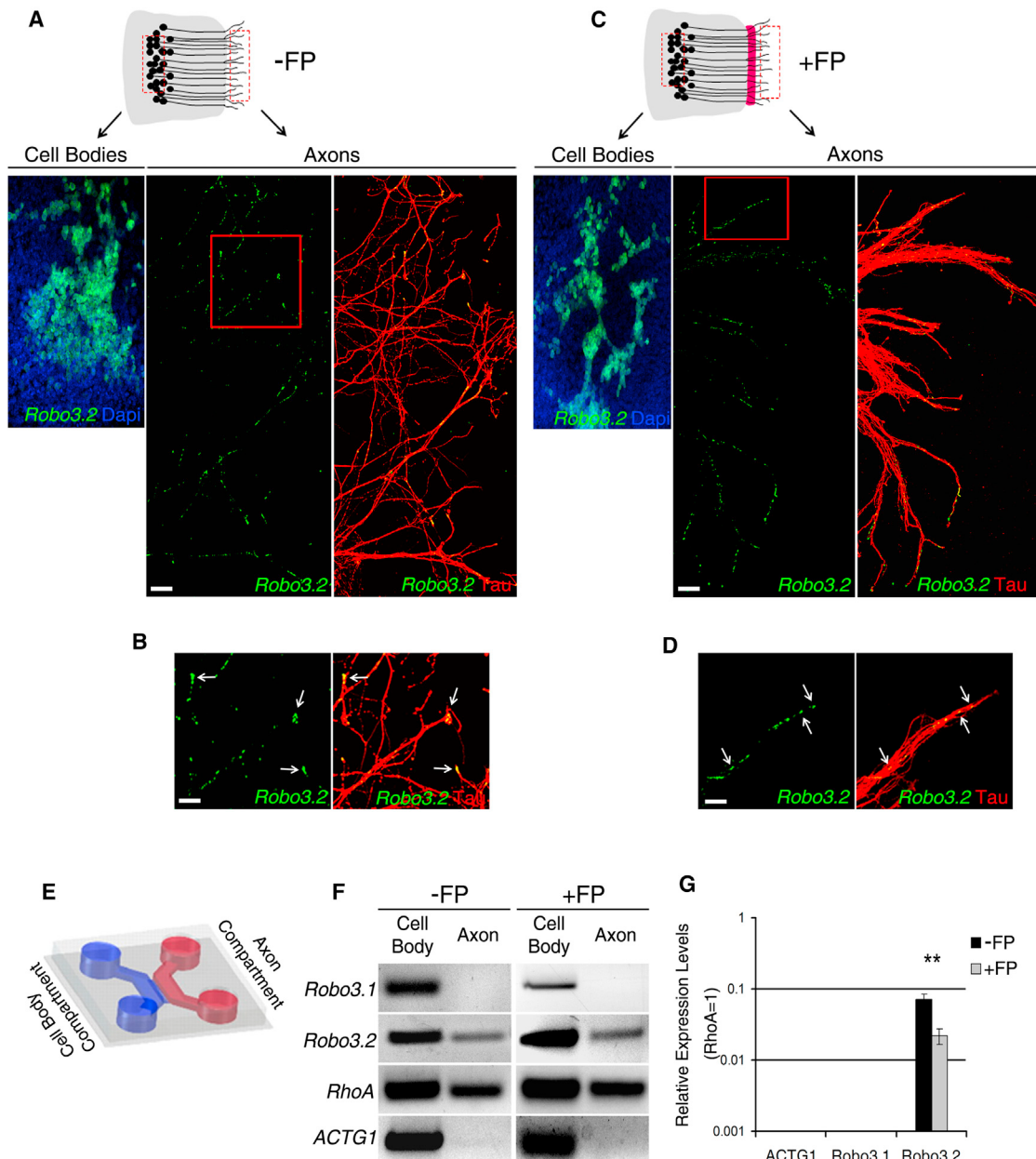


Figure 3. Robo3.2 mRNA Is Transported into Pre- and Postcrossing Commissural Axons

(A–D) Detection by FISH of endogenous *Robo3.2* mRNA in commissural axons. Antisense riboprobes against *Robo3.2* mRNA resulted in punctate labeling along axons in both –FP (A and B) and +FP (C and D) explants. Tau (red) immunolabeling was used to visualize axons. High-power images show prominent labeling at the distal tips of the axons (B and D, indicated by arrows). Scale bars: (A and C, axons) 150 μ m, (A and C, cell bodies) 60 μ m, (B and D) 60 μ m.

(E) Schematic of a microfluidic chamber that is used to isolate commissural axons from half-open-book explants. Half-open-book explants were cultured in the cell-body compartment. The microgrooves in microfluidic devices ensure that no cell bodies enter into the axonal compartment.

(F) Detection by RT-PCR of endogenous *Robo3.2* mRNA in purified commissural axons. *Robo3.2* transcripts were detected in axons of both –FP and +FP explants. *RhoA* mRNA and *gamma-actin* mRNA were used as positive and negative controls, respectively.

(G) Quantitative analysis of endogenous *Robo3.2* mRNA in purified –FP and +FP axons ($n = 3$ biological replicates; 65 explants/replicate). Consistent with the data in (F), *Robo3.2* mRNA is present in pre- and postcrossing axons. ** $p < 0.01$.

See also Figure S3.

downregulated when axons cross the midline (Chen et al., 2008), presumably via a transcriptional mechanism. FCM-mediated drop in *Robo3.1* levels was not affected by cycloheximide, as

this is not mediated by NMD (Figure 5A). These data suggest that *Robo3.2* mRNA becomes a substrate for NMD when its translation is induced.

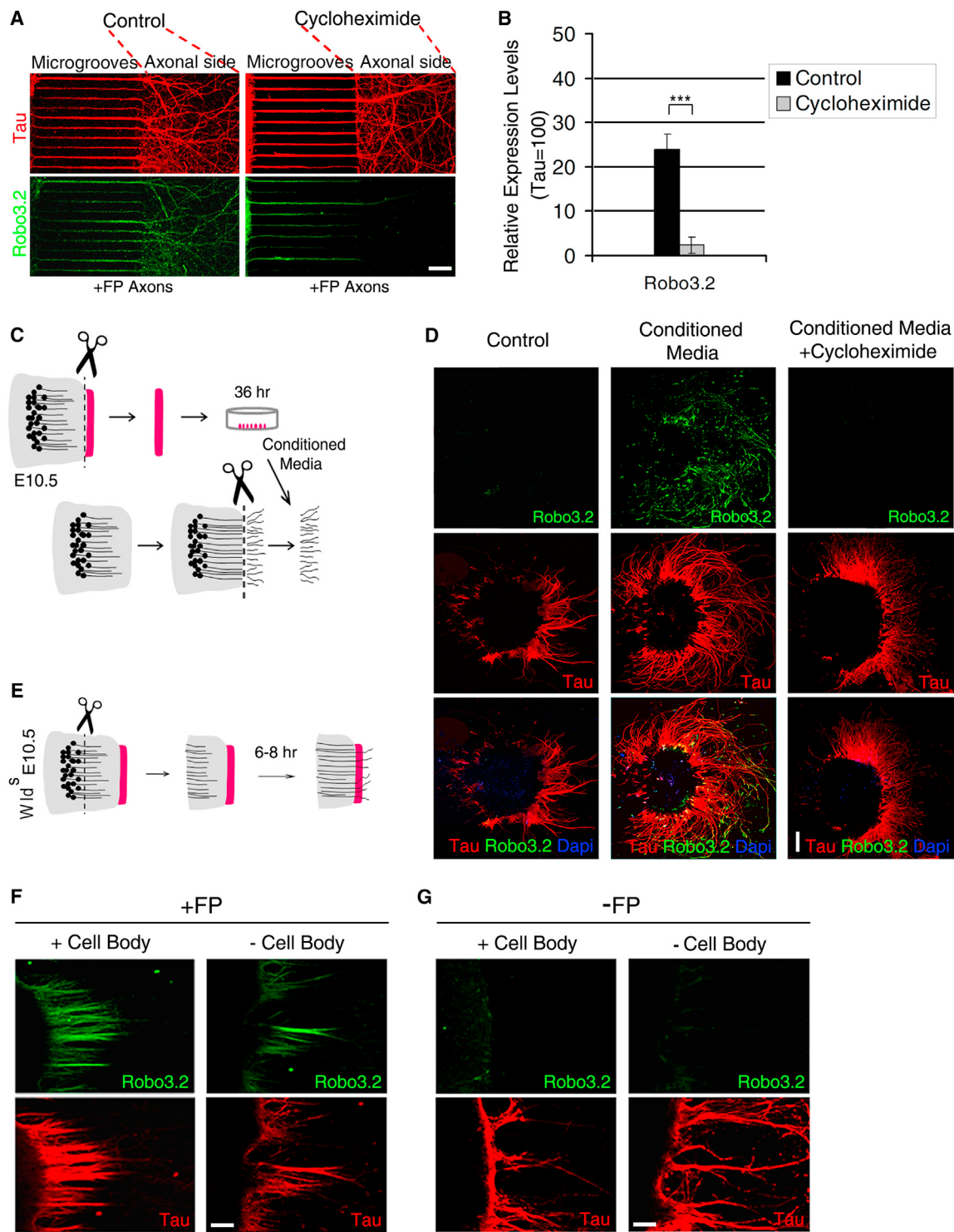


Figure 4. Robo3.2 Is Locally Translated in Commissural Axons

(A and B) Robo3.2 is locally translated in postcrossing axons. +FP explants were cultured in microfluidic chambers (A). Axonal treatment of cycloheximide (12 hr, 10 μ M) resulted in a more than 90% reduction in Robo3.2 protein levels in postcrossing axons ($n = 120$ axons/condition) (B). Data are represented as mean \pm SEM, *** $p < 0.001$.

(C and D) FCM induces local translation of Robo3.2. Schematic of the experimental design is shown (C). Application of FCM to severed -FP axons resulted in prominent axonal labeling of Robo3.2 protein (D). This effect was blocked by application of 10 μ M cycloheximide, indicating that Robo3.2 induction in axons is translation dependent.

(legend continued on next page)

To ensure that translation-dependent degradation of *Robo3.2* mRNA involves NMD, we repeated this experiment in NMD-deficient commissural neurons. We used *Upf2* conditional knockout (*Upf2* cKO) mouse (Weischenfeldt et al., 2008) expressing *Wnt1-Cre* to ablate *Upf2* expression selectively in dorsal commissural neurons (*Wnt1-Cre; Upf2^{f/f}*). We prepared -FP explants from *Wnt1-Cre; Upf2^{f/f}* (*Upf2* cKO) embryos and treated these explants with FCM (Figure S5B). Unlike in control explants (Figure 5A), FCM did not result in decreased *Robo3.2* transcript levels in NMD-deficient neurons. This confirms that *Robo3.2* degradation occurs in an NMD-dependent manner. Taken together, these experiments indicate that *Robo3.2* mRNA becomes a substrate for NMD when its translation is induced in axons.

NMD Components Are Enriched in Axonal Growth Cones

We next examined whether axons have the capacity to utilize NMD. NMD components have not been previously described in axons. Staining of distal commissural axons with antibodies specific for *Upf2* and *Upf1* revealed selective labeling of distal axons (Figures 5B and 5C). As with *Upf1* and *Upf2*, staining with an antibody specific for *Smg1*, a kinase required for NMD, revealed selective enrichment in the distal-most portion of these axons (Figure 5D). Western blot of these proteins in isolated axons further confirmed that commissural axons contain components of NMD machinery (Figure S5F). Taken together, these findings suggest that NMD might have functional roles in commissural axons.

NMD Regulates Robo3.2 Protein Levels in Postcrossing Axons

We first examined whether NMD is required for the floor-plate-dependent induction of *Robo3.2*. As with control explants, -FP explants exhibited minimal and +FP explants exhibited readily detectable *Robo3.2* expression in *Upf2* cKO embryos (Figures S5G and S5H), indicating that NMD is not involved in either repression or induction of *Robo3.2* during midline crossing.

We next examined whether NMD affects the levels of *Robo3.2* expression in commissural axons. We examined the effect of *Upf2* cKO on the levels of *Robo3.2* protein induction following treatment with FCM. -FP explants from both control and *Upf2* cKO embryos were treated with FCM, and *Robo3.2* levels were measured by immunofluorescence (Figures 5E and 5F). Following treatment with FCM, *Robo3.2* was induced in axons from both control and *Upf2* cKO explants (Figure 5E). However, *Robo3.2* staining was nearly 2-fold increased in axons from *Upf2* cKO explants (Figure 5F). This effect was also observed in transected axons that received FCM, confirming that the increase in *Robo3.2* derives from local translation (Figures 5G and S6A–S6B').

(E–G) *Robo3.2* is locally translated in postcrossing axons in the absence of commissural cell bodies. (E) shows a schematic representation of the experimental design. +FP axons from *Wld^S* mice were assayed to monitor *Robo3.2* in spinal-cord explants in which the cell bodies were transected from the axons before axons reach the midline. Severed axons from *Wld^S* grew through the floor plate with no degeneration. Severed axons induced *Robo3.2* protein after crossing the midline in the absence of cell bodies (F, right panels).

Scale bars: (A) 75 μm, (D) 200 μm, (F and G) 60 μm. See also Figure S4.

We next monitored *Robo3.2* expression in axons that contact the floor plate in *Upf2* cKO explants. Contact with the floor plate provides a more physiologically relevant stimulus than FCM. Staining of axons from +FP explants indicated that *Robo3.2* levels were 3.5-fold higher in *Upf2* cKO explants compared to controls (Figures 5H and 5I). Taken together, these data indicate that NMD limits the amount of *Robo3.2* protein in axons exposed to floor-plate signals.

We next asked whether the higher *Robo3.2* levels in axons are due to increased stability of *Robo3.2* mRNAs in axons. We measured *Robo3.2* mRNA levels in axons from control and *Upf2* cKO explants. We treated -FP axons of control and *Upf2* cKO explants in microfluidic chambers with FCM (Figure 5J). We also used NMD-deficient axons by testing isolated +FP axons from *Upf2* cKO explants (Figure 5J). In both cases, *Robo3.2* mRNA levels were found to be higher in *Upf2* cKO axons compared to control axons. Taken together, these data indicate that axonal *Robo3.2* transcripts are degraded by NMD, which limits *Robo3.2* protein levels in postcrossing axons.

As a control, we examined whether the increased levels of *Robo3.2* protein in *Upf2* cKO commissural axons could be due to an overall increase in the level of *Robo3.2* mRNA in cell bodies. We measured *Robo3.2* mRNA levels in control and *Upf2* cKO commissural cell bodies at E13.5. *Robo3.2* mRNA levels were not significantly affected in the *Upf2* cKO commissural cell bodies compared to controls (Figure S6C). These data are consistent with the idea that the upregulation of *Robo3.2* protein in *Upf2*-deficient axons is not due to an overall increase in *Robo3.2* mRNA levels in cell bodies (Figure S6C).

NMD Regulates Postcrossing Axon Behavior

We next sought to investigate whether NMD influences commissural axon guidance during development. Dorsal commissural axons are initially attracted to the midline. After crossing the midline, they exert a more complicated trajectory with respect to the distance from the midline (Kadison and Kaprielian, 2004). Whereas only a small portion of the postcrossing axons (medial longitudinal commissural, MLC) remain adjacent to the midline, the majority (intermediate longitudinal commissural, ILC) travel away from the midline and project diagonally before ascending in the spinal cord (Jaworski et al., 2010; Kadison and Kaprielian, 2004) (Figure 6A).

To address the potential function of NMD in commissural axon guidance, we analyzed commissural axon trajectories in *Upf2* cKO embryos. To assess axon trajectories, the lipophilic tracer Dil was injected into E13.5 spinal cords, and axons were analyzed after the entire axon was uniformly labeled with Dil. *Upf2* cKO axons exhibited normal precrossing behavior but displayed more lateral trajectories on the contralateral side compared to control axons (Figure 6B). To measure the lateral distribution, the ascending axons were binned into three categories based on their distances from the midline: 0–75 μm, 75–275 μm,

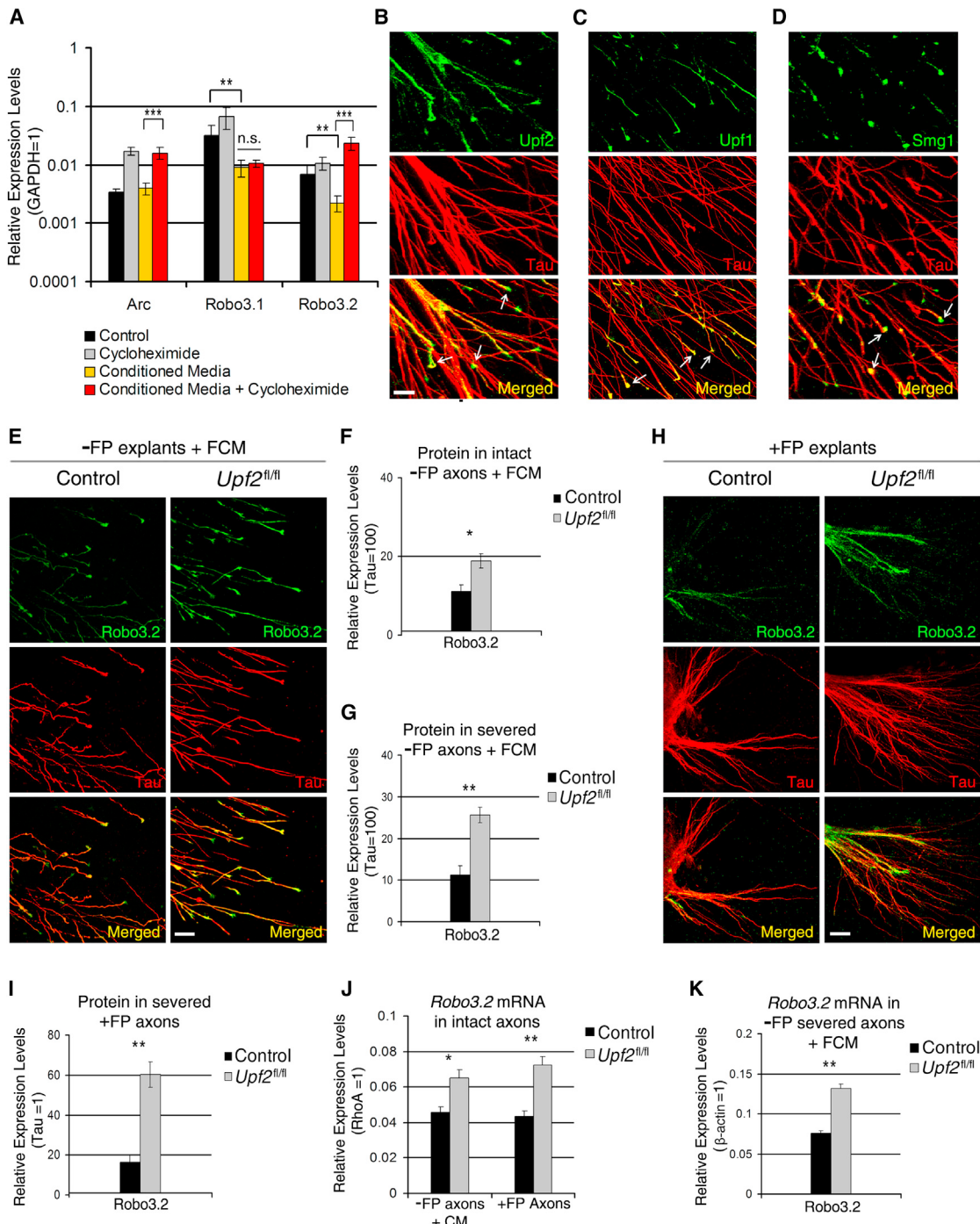


Figure 5. NMD Regulates Robo3.2 Protein Levels in Postcrossing Commissural Axons

(A) Robo3.2 mRNA becomes a target of NMD following exposure to FCM. FCM resulted in 70% lower levels of Robo3.2 mRNA in commissural cell bodies compared to control-treated explants. This reduction was blocked by treatment with 10 μ M cycloheximide, suggesting that Robo3.2 degradation upon FCM is NMD dependent.

(B–D) Upf2 (B), Upf1 (C), and Smg1 (D) are localized to axons, with increased levels at axonal tips.

(E) FCM treatment resulted in higher Robo3.2 levels in –FP axons from Upf2 cKO explants compared to –FP axons from control.

(F) Quantifications of results in (E) (110 axons per control [n = 3] and mutant [n = 4] embryos).

(G) Quantification of Robo3.2 protein in severed axons following treatment with FCM (460 control axons [n = 11 explants, 4 embryos] and 410 Upf2 cKO axons [n = 10 explants, 3 embryos]). (See also Figures S6A and S6B.)

(H) Robo3.2 immunostaining in +FP axons from control and Upf2 cKO.

(legend continued on next page)

and >275 μm (Figures 6A and 6B). In *Upf2* cKO embryos, the proportions of postcrossing axons in the 0–75 μm and 75–275 μm categories were significantly reduced, whereas the proportion in the >275 μm category was significantly increased (Figure 6C). Additionally, *Upf2* cKO axons exhibited disorganized trajectories with several sudden turns and path changes (Figure 6D).

To further confirm the phenotype of NMD-deficient neurons, we electroporated a dominant-negative *Upf1* construct, (h*Upf1* K498A) in E10.5 open-book explants (Figure 6E). As with the *Upf2* cKO neurons, expression of dominant-negative *Upf1* resulted in lateral positioning of the axonal trajectories (Figures 6F and 6G). The increased lateral distribution of postcrossing axons is consistent with over-repulsion from the midline due to excessive levels of Robo3.2. Taken together, these data indicate that NMD is required for the proper guidance of postcrossing axons.

Because Robo1 and Robo2 influence postcrossing trajectories, we asked whether their expression was altered in *Upf2* cKO axons. qRT-PCR showed that *Robo1* and *Robo2* transcripts are not affected in *Upf2* cKO neurons compared to control neurons (Figure S6D), suggesting that misregulation of Robo1 and Robo2 is unlikely to contribute to the guidance defects in NMD-deficient neurons.

Localization of NMD Machinery in Growth Cones Is a Feature of Various Types of Neurons

We next asked whether local regulation of mRNA stability by NMD could occur in axons of other neuronal types. We performed immunostainings for *Upf2*, *Upf1*, and Smg1 on postnatal day 1 (P1) DIV7 rat hippocampal and E14 rat dorsal root ganglia (DRG) neurons (Figure 7). Similar to commissural neurons, all of these proteins were highly enriched in growth cones of both neuronal types (Figure 7C).

Although Robo3 has major roles in the guidance of commissural axons, Robo3 is not expressed in many neurons and has no described functions in hippocampal and sensory neurons (Sabatier et al., 2004). However, other NMD targets are likely to exist in neurons. For example, at least 152 predicted NMD targets were predicted based on the presence of spliced introns in the 3' UTR (Giorgi et al., 2007). These data suggest that the local utilization of NMD to regulate mRNA stability and protein levels in growth cones may be a common feature of diverse neuronal types.

DISCUSSION

Our study identifies intra-axonal NMD as a mechanism that regulates axon guidance. We find that proteins that are involved in NMD display substantial enrichment in growth cones in various diverse types of neurons. This localization suggests that NMD

may function locally within growth cones to regulate local protein expression. Our data indicate that NMD regulates the levels of Robo3.2 in growth cones and thereby influences the chemo-tropic properties of growth cones and their axonal trajectories after midline crossing.

Role of NMD in Regulating Robo3.2 and Postcrossing Axon Trajectories

Our data demonstrate that transcripts can evade NMD by translational repression. Our polysome-profiling experiments suggest that *Robo3.2* transcripts are translationally repressed in cell bodies and precrossing axons. When the axon encounters the floor plate, *Robo3.2* is derepressed, resulting in local synthesis and enabling surveillance by the NMD machinery within the distal axon. Thus the initial round of translation, which typically occurs on nascent mRNA, occurs locally within axons after *Robo3.2* is translationally derepressed by the floor plate (Figure S7C). NMD-dependent degradation of *Robo3.2* transcripts limits Robo3.2 levels, potentially to a single Robo3.2 per targeted mRNA.

Our data indicate that the proper guidance of postcrossing commissural axons requires NMD. NMD-deficient postcrossing axons exhibit elevated Robo3.2 levels and over-repulsion from the midline in vivo. This is consistent with previous studies showing that overexpression of Robo3.2 in precrossing neurons leads to repulsion of axons from the midline (Chen et al., 2008). NMD-dependent control of Robo3.2 levels is likely to contribute to the overall level of axonal repulsion from the midline, ensuring proper lateral positioning of the axons during ascension in the spinal cord. However, NMD is likely to have additional targets in axons. Cell-adhesion molecules and cytoskeletal molecules are known to regulate axon guidance (Vitriol and Zheng, 2012). Conceivably, physiological regulation of transcripts encoding these or other proteins by axonal NMD may influence axonal trajectories.

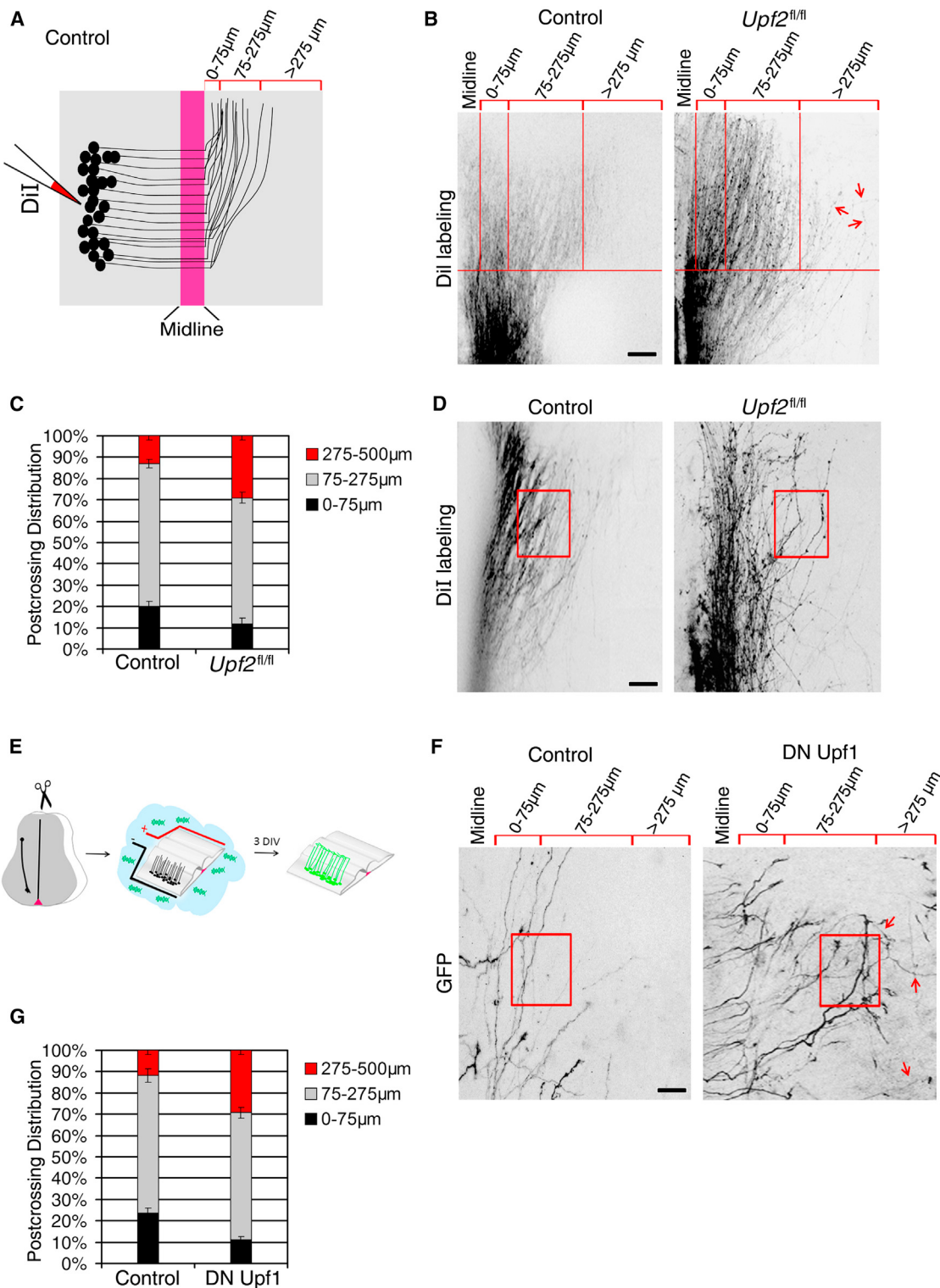
Potential Role of Robo3.2 in Postcrossing Axons of Dorsal Commissural Neurons

Axons of dorsal commissural neurons sort into specific mediolateral positions in the contralateral side after crossing the midline (Imondi and Kaprielian, 2001; Jaworski et al., 2010; Kadison and Kaprielian, 2004). Whereas the minority of the postcrossing axons remain in the longitudinal track adjacent to the midline (MLC), the majority project diagonally away from the midline to varying lateral positions (ILC). We find that the absence of NMD results in a reduction in MLC trajectories, consistent with them adopting a more diagonal trajectory, as well as a lateral shift in the ILC trajectories. These trajectory shifts are consistent with over-repulsion from the midline.

(I) Robo3.2 is 3.5-fold higher in postcrossing axons of *Upf2* cKO compared to control axons (211 axons, control [n = 11 axonal areas, 4 embryos] and 217 axons, mutant [n = 13 axonal areas, 5 embryos]).

(J and K) Quantification by qRT-PCR of *Robo3.2* mRNA in isolated unsevered (J) and severed (K) axons following induction of *Robo3.2* translation by FCM. Axons were harvested from control and *Upf2* cKO explants that were cultured in microfluidic chambers. Both *Upf2* cKO –FP axons that were treated with FCM and *Upf2* cKO +FP axons that encountered the floor plate have higher levels of *Robo3.2* mRNA compared to control axons (J) (*Upf2* cKO –FP axons [n = 38 explants, 5 embryos], control –FP axons [n = 30 explants, 4 embryos], *Upf2* cKO +FP axons [n = 41 explants, 5 embryos], and control +FP axons [n = 35 explants, 4 embryos]). qRT-PCR is shown for *Robo3.2* mRNA in isolated, –FP severed axons following FCM treatment (K) (74 control [n = 3 embryos] and 77 *Upf2* cKO [n = 3 embryos]).

Data are represented as mean ± SEM, *p < 0.05, **p < 0.01, and ***p < 0.001. Scale bars: (B–D) 75 μm, (E and H) 100 μm. See also Figures S5 and S6.

**Figure 6. NMD Regulates Postcrossing Axon Behavior**

(A) Schematic of precrossing and postcrossing axon behavior. Axons were visualized by Dil at E13.5. Postcrossing axons were binned into three categories based on their distance from midline: 0–75 μ m, 75–275 μ m, and >275 μ m.

(B) *Upf2* cKO axons exhibited normal precrossing behavior but more lateral postcrossing trajectories than control axons.

(C) Many more *Upf2* cKO axons are seen >275 μ m from the midline compared to control axons (459 axons, control [n = 5] and 559 axons, *Upf2* cKO [n = 6]).

(legend continued on next page)

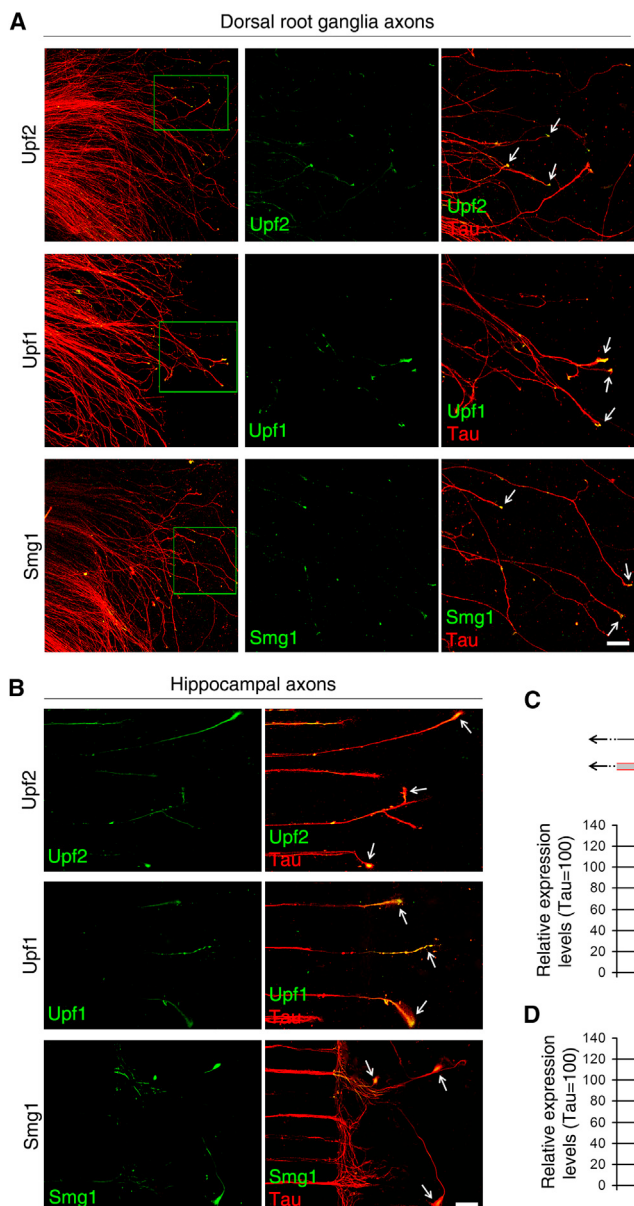


Figure 7. NMD Machinery Is Localized to Growth Cones of Several Types of Neurons
(A and B) Upf2, Upf1, and Smg1 localize to axons and growth cones of peripheral (A) and central (B) nervous system neurons.

(C and D) Quantifications of the fluorescence intensities of NMD proteins in individual axons of dorsal root ganglia (C) and hippocampal (D) neurons.

Data are represented as mean \pm SEM. Scale bars: (A) 100 μm , (B) 30 μm .

given that knockdown of Robo3.2 reduces Robo1/2-mediated repulsion from the midline (Chen et al., 2008). However, it is not clear what determines the degree of the repulsion from the midline during diagonal trajectories. Our findings suggest the possibility that the level of Robo3.2 in postcrossing axons may determine the degree of repulsion from the midline. Although the MLC axons and ILC axons in close proximity to the midline might have moderate levels of Robo3.2, the more lateral ILC axons may have higher Robo3.2, ensuring proper lateral positioning. An intriguing possibility is that the level of NMD activity may vary in different axons, resulting in different levels of axonal Robo3.2 and lateral positioning.

Local NMD as a Regulator of Local Translation

We also find that the growth cone is a site for local NMD in neurons. NMD has previously been shown to regulate the expression of *Arc* transcripts in hippocampal neurons in response to synaptic stimulation (Giorgi et al., 2007). However, the possibility of local regulation of *Arc* transcripts by NMD within dendrites or spines was not examined. Our data suggest that

NMD can function locally to regulate the translation of local mRNA pools. Conceivably, NMD may have important roles in the regulation of local translation pathways in dendritic spines, which are regions that are also characterized by high levels of local translation (Bramham and Wells, 2007; Sutton and Schuman, 2006). The high degree of enrichment of NMD proteins in growth cones suggests that NMD may influence axonal mRNAs that affect various growth-cone functions. Apart from NMD, Upf1 is also involved in Staufen1-mediated mRNA decay (SMD)

During midline crossing, Robo proteins contribute to distinct guidance decisions (Evans and Bashaw, 2010; Jaworski et al., 2010; Spitzweck et al., 2010). Robo1 ensures that all commissural axons leave the midline, whereas Robo2 is required for the initiation of the diagonal trajectories in mouse spinal cord (Jaworski et al., 2010; Reeber et al., 2008). The role of Robo2 in diagonal trajectories is supported by the finding that postcrossing axons remain adjacent to the midline in *Robo2*^{-/-} spinal cord. Robo3.2 appears to enhance the activity of Robo2

(E) Schematic of electroporation in spinal-cord open-book cultures.

(F) Electroporation of dominant-negative Upf1 in commissural neurons resulted in aberrant guidance similar to that in *Upf2* cKO axons.

(G) Lateral distributions of postcrossing axons following dominant-negative Upf1 electroporation (153 axons, control [n = 4] and 131 axons, *Upf2* cKO [n = 3]). Data are represented as mean \pm SEM. Scale bars: (B) 200 μm , (D and F) 75 μm .

(Kim et al., 2005). Thus, axonally localized Upf1 may also influence the translation of SMD targets.

Our data demonstrate that local translation is regulated by mechanisms that control mRNA stability in axons. Pathways that induce mRNA degradation can limit the total amount of protein that can be translated. The expression of NMD proteins in growth cones of diverse neuronal types suggests that this may be a recurrent mechanism used to influence local translation pathways.

Local Translation Regulates the Pathfinding Behavior of Growth Cones at the Floor Plate

Our data also provide insight into the mechanism by which the floor plate alters chemotropic responses of axons. A previous study by Flanagan and colleagues (Brittis et al., 2002) initially raised the possibility that local translation could affect the chemotropic properties of growth cones by showing that the midline could induce the translation of a reporter construct containing the 3' UTR of *EphA2*. However, the endogenous *EphA2* transcript was not detected in commissural axons, and no endogenous transcripts that are translated in response to exposure to the floor plate were identified. Our data demonstrate an endogenous transcript that is locally translated in response to the floor plate.

It remains unclear which floor-plate-derived factor triggers axonal translation of *Robo3.2*. Well-known floor-plate cues netrin-1, sonic hedgehog, and NrCAM do not induce *Robo3.2* protein in commissural axons (D.C. and S.R.J., unpublished data). Because FCM is capable of inducing *Robo3.2* synthesis, the responsible factor may be a secreted molecule. However, FCM may contain ectodomains of surface or transmembrane proteins shed following cleavage by membrane-associated proteases. Indeed, a recent study found that the transmembrane protein NrCAM accumulates in FCM (Nawabi et al., 2010). Therefore, physiologic induction of *Robo3.2* synthesis may be mediated by contact of axons with membrane-bound proteins in floor-plate cells.

EXPERIMENTAL PROCEDURES

Mice and Constructs

Explant cultures were prepared from CD1 mouse embryos (Charles River Laboratories), *Upf2* cKO mice (Weischenfeldt et al., 2008), or C57BL/6OlaHsd-Wld^s mice (Harlan). In experiments with *Upf2* deletion in commissural neurons, *Upf2* cKO mice were crossed with *Wnt1-Cre* mice (Matsumoto et al., 2007), and *Wnt1-Cre; Upf2^{fl/fl}* or *Wnt1-Cre; Upf2^{w/w}* embryos were used. The hUpf1 K498A dominant-negative expression vector was a gift from Jens Lykke-Andersen (University of California, San Diego, CA, USA) and was coelectroporated with an EGFP-expressing plasmid in order to identify the transfected neurons.

Explant Cultures and Reagents

Open-book explant cultures were prepared from E10.5 thoracic spinal cords as previously described (Moore and Kennedy, 2008). FCM was prepared by culturing thoracic spinal cord floor plate from 20 E10.5 embryos (200 explants) in 300 μ l Neurobasal media. The conditioned medium was collected after 36 hr, and the entire 300 μ l was applied to axons. Microfluidic chambers were prepared as described previously (Cohen et al., 2011; Hengst et al., 2009; Taylor et al., 2005). For additional details, see the Extended Experimental Procedures.

Immunofluorescence, RNA Preparation, and Expression Analysis

Half-open-book explants were fixed in 4% paraformaldehyde prior to immunostaining with antibodies specific to Robo3.1 and Robo3.2 (Genentech). Immunofluorescence was acquired on a Zeiss LSM 510 confocal microscopy and processed with LSM 5 image examiner. RNA was prepared with TRIzol (Invitrogen). RT-PCR was performed with SuperScript III (Invitrogen). For additional details, see the Extended Experimental Procedures.

Data Analysis

Statistical analysis was performed with Student's t test and is reported as mean \pm standard error of the mean (SEM). When comparing different treatments on wild-type explants, we considered the samples as two samples with equal variance. When comparing mutant tissue with control littermates, we considered the samples as two samples with unequal variance. In all cases, a two-tailed distribution parameter was applied.

SUPPLEMENTAL INFORMATION

Supplemental Information includes Extended Experimental Procedures and seven figures and can be found with this article online at <http://dx.doi.org/10.1016/j.cell.2013.04.056>.

ACKNOWLEDGMENTS

We thank J. Lykke-Andersen for generously providing the hUpf1 K498A construct and anti-Upf1 and anti-Upf2 antibodies, S. Blanchard and L. Wang for equipment and helpful suggestions regarding the polysome experiments, S. Kadison for advice on Dil labeling, and M. Tessier-Lavigne and Genentech for sharing Robo3.1- and Robo3.2-specific antibodies. We also thank members of the Jaffrey lab for helpful comments and suggestions. This work was supported by NIH grant NS56306 to S.R.J. and a European Molecular Biology Organization (EMBO) postdoctoral fellowship to D.C.

Received: September 11, 2012

Revised: March 5, 2013

Accepted: April 30, 2013

Published: June 6, 2013

REFERENCES

- Black, D.L., and Zipursky, S.L. (2008). To cross or not to cross: alternatively spliced forms of the Robo3 receptor regulate discrete steps in axonal midline crossing. *Neuron* 58, 297–298.
- Bramham, C.R., and Wells, D.G. (2007). Dendritic mRNA: transport, translation and function. *Nat. Rev. Neurosci.* 8, 776–789.
- Brittis, P.A., Lu, Q., and Flanagan, J.G. (2002). Axonal protein synthesis provides a mechanism for localized regulation at an intermediate target. *Cell* 110, 223–235.
- Campbell, D.S., and Holt, C.E. (2001). Chemotropic responses of retinal growth cones mediated by rapid local protein synthesis and degradation. *Neuron* 32, 1013–1026.
- Carter, M.S., Doskow, J., Morris, P., Li, S., Nhim, R.P., Sandstedt, S., and Wilkinson, M.F. (1995). A regulatory mechanism that detects premature nonsense codons in T-cell receptor transcripts *in vivo* is reversed by protein synthesis inhibitors *in vitro*. *J. Biol. Chem.* 270, 28995–29003.
- Chang, Y.F., Imam, J.S., and Wilkinson, M.F. (2007). The nonsense-mediated decay RNA surveillance pathway. *Annu. Rev. Biochem.* 76, 51–74.
- Chen, Z., Gore, B.B., Long, H., Ma, L., and Tessier-Lavigne, M. (2008). Alternative splicing of the Robo3 axon guidance receptor governs the midline switch from attraction to repulsion. *Neuron* 58, 325–332.
- Cohen, M.S., Bas Orth, C., Kim, H.J., Jeon, N.L., and Jaffrey, S.R. (2011). Neuregulin-mediated dendrite-to-nucleus signaling revealed by microfluidic compartmentalization of dendrites. *Proc. Natl. Acad. Sci. USA* 108, 11246–11251.

- Doma, M.K., and Parker, R. (2007). RNA quality control in eukaryotes. *Cell* **131**, 660–668.
- Dostie, J., and Dreyfuss, G. (2002). Translation is required to remove Y14 from mRNAs in the cytoplasm. *Curr. Biol.* **12**, 1060–1067.
- Evans, T.A., and Bashaw, G.J. (2010). Functional diversity of Robo receptor immunoglobulin domains promotes distinct axon guidance decisions. *Curr. Biol.* **20**, 567–572.
- Feng, Y., Yan, T., He, Z., and Zhai, Q. (2010). Wld(S), Nmnats and axon degeneration—progress in the past two decades. *Protein Cell* **1**, 237–245.
- Giorgi, C., Yeo, G.W., Stone, M.E., Katz, D.B., Burge, C., Turrigiano, G., and Moore, M.J. (2007). The EJC factor eIF4AIII modulates synaptic strength and neuronal protein expression. *Cell* **130**, 179–191.
- Hengst, U., Deglincerti, A., Kim, H.J., Jeon, N.L., and Jaffrey, S.R. (2009). Axonal elongation triggered by stimulus-induced local translation of a polarity complex protein. *Nat. Cell Biol.* **11**, 1024–1030.
- Hodgkin, J., Papp, A., Pulak, R., Ambros, V., and Anderson, P. (1989). A new kind of informational suppression in the nematode *Caenorhabditis elegans*. *Genetics* **123**, 301–313.
- Imondi, R., and Kaprielian, Z. (2001). Commissural axon pathfinding on the contralateral side of the floor plate: a role for B-class ephrins in specifying the dorsoventral position of longitudinally projecting commissural axons. *Development* **128**, 4859–4871.
- Ishigaki, Y., Li, X., Serin, G., and Maquat, L.E. (2001). Evidence for a pioneer round of mRNA translation: mRNAs subject to nonsense-mediated decay in mammalian cells are bound by CBP80 and CBP20. *Cell* **106**, 607–617.
- Jaworski, A., Long, H., and Tessier-Lavigne, M. (2010). Collaborative and specialized functions of Robo1 and Robo2 in spinal commissural axon guidance. *J. Neurosci.* **30**, 9445–9453.
- Jung, H., Yoon, B.C., and Holt, C.E. (2012). Axonal mRNA localization and local protein synthesis in nervous system assembly, maintenance and repair. *Nat. Rev. Neurosci.* **13**, 308–324.
- Kadison, S.R., and Kaprielian, Z. (2004). Diversity of contralateral commissural projections in the embryonic rodent spinal cord. *J. Comp. Neurol.* **472**, 411–422.
- Kim, Y.K., Furic, L., Desgroseillers, L., and Maquat, L.E. (2005). Mammalian Staufen1 recruits Upf1 to specific mRNA 3'UTRs so as to elicit mRNA decay. *Cell* **120**, 195–208.
- Leeds, P., Wood, J.M., Lee, B.S., and Culbertson, M.R. (1992). Gene products that promote mRNA turnover in *Saccharomyces cerevisiae*. *Mol. Cell. Biol.* **12**, 2165–2177.
- Lejeune, F., and Maquat, L.E. (2005). Mechanistic links between nonsense-mediated mRNA decay and pre-mRNA splicing in mammalian cells. *Curr. Opin. Cell Biol.* **17**, 309–315.
- Leung, K.M., van Horck, F.P., Lin, A.C., Allison, R., Standart, N., and Holt, C.E. (2006). Asymmetrical beta-actin mRNA translation in growth cones mediates attractive turning to netrin-1. *Nat. Neurosci.* **9**, 1247–1256.
- Li, S., and Wilkinson, M.F. (1998). Nonsense surveillance in lymphocytes? *Immunity* **8**, 135–141.
- Long, H., Sabatier, C., Ma, L., Plump, A., Yuan, W., Ornitz, D.M., Tamada, A., Murakami, F., Goodman, C.S., and Tessier-Lavigne, M. (2004). Conserved roles for Slit and Robo proteins in midline commissural axon guidance. *Neuron* **42**, 213–223.
- Maquat, L.E., Kinniburgh, A.J., Rachmilewitz, E.A., and Ross, J. (1981). Unstable beta-globin mRNA in mRNA-deficient beta 0 thalassemia. *Cell* **27**, 543–553.
- Matsumoto, Y., Irie, F., Inatani, M., Tessier-Lavigne, M., and Yamaguchi, Y. (2007). Netrin-1/DCC signaling in commissural axon guidance requires cell-autonomous expression of heparan sulfate. *J. Neurosci.* **27**, 4342–4350.
- McGlincy, N.J., and Smith, C.W. (2008). Alternative splicing resulting in nonsense-mediated mRNA decay: what is the meaning of nonsense? *Trends Biochem. Sci.* **33**, 385–393.
- Moore, S.W., and Kennedy, T.E. (2008). Dissection and culture of embryonic spinal commissural neurons. In *Current Protocols in Neuroscience*, Chapter 3, Unit 3.20. <http://dx.doi.org/10.1002/0471142301.ns0320s45>.
- Nawabi, H., Briançon-Marjollet, A., Clark, C., Sanyas, I., Takamatsu, H., Okuno, T., Kumanogoh, A., Bozon, M., Takeshima, K., Yoshida, Y., et al. (2010). A midline switch of receptor processing regulates commissural axon guidance in vertebrates. *Genes Dev.* **24**, 396–410.
- O'Donnell, M., Chance, R.K., and Bashaw, G.J. (2009). Axon growth and guidance: receptor regulation and signal transduction. *Annu. Rev. Neurosci.* **32**, 383–412.
- Perry, V.H., Brown, M.C., and Lunn, E.R. (1991). Very slow retrograde and Wallerian degeneration in the CNS of C57BL/6 mice. *Eur. J. Neurosci.* **3**, 102–105.
- Reeber, S.L., Sakai, N., Nakada, Y., Dumas, J., Dobrenis, K., Johnson, J.E., and Kaprielian, Z. (2008). Manipulating Robo expression in vivo perturbs commissural axon pathfinding in the chick spinal cord. *J. Neurosci.* **28**, 8698–8708.
- Sabatier, C., Plump, A.S., Le, M., Brose, K., Tamada, A., Murakami, F., Lee, E.Y., and Tessier-Lavigne, M. (2004). The divergent Robo family protein rig-1/Robo3 is a negative regulator of slit responsiveness required for midline crossing by commissural axons. *Cell* **117**, 157–169.
- Serafini, T., Kennedy, T.E., Gallo, M.J., Mirzayan, C., Jessell, T.M., and Tessier-Lavigne, M. (1994). The netrins define a family of axon outgrowth-promoting proteins homologous to *C. elegans* UNC-6. *Cell* **78**, 409–424.
- Spitzweck, B., Brankatschk, M., and Dickson, B.J. (2010). Distinct protein domains and expression patterns confer divergent axon guidance functions for *Drosophila* Robo receptors. *Cell* **140**, 409–420.
- Sutton, M.A., and Schuman, E.M. (2006). Dendritic protein synthesis, synaptic plasticity, and memory. *Cell* **127**, 49–58.
- Taylor, A.M., Burton-Jones, M., Rhee, S.W., Cribbs, D.H., Cotman, C.W., and Jeon, N.L. (2005). A microfluidic culture platform for CNS axonal injury, regeneration and transport. *Nat. Methods* **2**, 599–605.
- Tennyson, V.M. (1970). The fine structure of the axon and growth cone of the dorsal root neuroblast of the rabbit embryo. *J. Cell Biol.* **44**, 62–79.
- Vitriol, E.A., and Zheng, J.Q. (2012). Growth cone travel in space and time: the cellular ensemble of cytoskeleton, adhesion, and membrane. *Neuron* **73**, 1068–1081.
- Weischenfeldt, J., Damgaard, I., Bryder, D., Theilgaard-Mönch, K., Thoren, L.A., Nielsen, F.C., Jacobsen, S.E., Nerlov, C., and Porse, B.T. (2008). NMD is essential for hematopoietic stem and progenitor cells and for eliminating by-products of programmed DNA rearrangements. *Genes Dev.* **22**, 1381–1396.
- Weischenfeldt, J., Waage, J., Tian, G., Zhao, J., Damgaard, I., Jakobsen, J.S., Kristiansen, K., Krogh, A., Wang, J., and Porse, B.T. (2012). Mammalian tissues defective in nonsense-mediated mRNA decay display highly aberrant splicing patterns. *Genome Biol.* **13**, R35.
- Zhang, J., Sun, X., Qian, Y., LaDuca, J.P., and Maquat, L.E. (1998). At least one intron is required for the nonsense-mediated decay of triosephosphate isomerase mRNA: a possible link between nuclear splicing and cytoplasmic translation. *Mol. Cell. Biol.* **18**, 5272–5283.
- Zheng, S., Gray, E.E., Chawla, G., Porse, B.T., O'Dell, T.J., and Black, D.L. (2012). PSD-95 is post-transcriptionally repressed during early neural development by PTBP1 and PTBP2. *Nat. Neurosci.* **15**, 381–388, S1.
- Zou, Y., Stoeckli, E., Chen, H., and Tessier-Lavigne, M. (2000). Squeezing axons out of the gray matter: a role for slit and semaphorin proteins from midline and ventral spinal cord. *Cell* **102**, 363–375.